Digital discrimination of neutron and γ ray using an organic scintillation detector based on wavelet transform modulus maximum *

YANG Yun(杨云) LIU Guo-Fu(刘国福) YANG Jun(杨俊)[1)]
LUO Xiao-Liang(罗晓亮) MENG De-Yuan(孟德远)
College of Mechatronics and Automation, National University of Defense Technology, Changsha 410073, China

Abstract: A novel algorithm for the discrimination of neutron and γ-ray events with wavelet transform modulus maximum (WTMM) in an organic scintillation has been investigated. Voltage pulses arising from a BC501A organic liquid scintillation detector in a mixed radiation field have been recorded with a fast digital sampling oscilloscope. The WTMM method using frequency-domain features exhibits a strong insensitivity to noise and can be used to discriminate neutron and γ-ray events based on their different asymptotic decay trend between the positive modulus maximum curve and the negative modulus maximum curve in the scale-space plane. This technique has been verified by the corresponding mixed-field data assessed by the time-of-flight (TOF) method and the charge comparison (CC) method. It is shown that the characterization of neutron and γ ray achieved by the discrimination method based on WTMM is consistent with that afforded by the TOF method and better than the CC method. Moreover, the WTMM method itself has presented its ability to eliminate the noise without any pretreatment to the pulses.

Key words: n/γ discrimination, organic scintillation, modulus maximum, TOF

PACS: 29.30.Hs, 29.40.Mc, 28.41.Rc **DOI:** 10.1088/1674-1137/38/3/036202

1 Introduction

Neutron detection technology has been widely used in the fields of explosive detection, environmental radiation detection, military and deep space exploration. Since almost all neutron fields coexist with an associated γ-ray component while neutron detectors are also sensitive to γ-ray photons, the discrimination between neutrons and γ rays (n/γ) becomes a key technical problem in the field of neutron detection [1]. Liquid scintillators are one of the most popular radiation detection materials because of their being shaped into the desired size for a specific application and their excellent pulse shape discrimination (PSD) properties and fast timing performance.

A number of existing techniques for PSD can be primarily assorted as time-based and frequency-based. As for time-based techniques, the most popular methods are charge comparison (CC) method [2, 3] and the zero-crossing method [4, 5]. Both of the methods were originally implemented in analogue electronics, often in dedicated instrumentation modules or nuclear instrument modules. More recently, they have been implemented in the digital domain as digital electronic platforms have become available with the requisite speed and cost to make this possible [6–8]. Currently these methods are the industrial standards to be used to compare with other new proposed discrimination methods, such as the pulse gradient analysis (PGA) [9–11] method, which is based on the comparison of the relative heights of samples in the trailing edge of the pulse, and curve-fitting method [12]. Since the scintillation process and the photomultiplier tube (PMT) anode signal are often very noisy and time-domain features are naturally highly dependent on the signal amplitude at specific time, these pulse shape discrimination methods can have a great dependency on the de-noising algorithm.

In recent years, the frequency-based techniques have emerged as a mature technology, with successful applications across many fields. They are particularly effective pattern recognition tools and can be used to classify neutron and γ-ray events from the measurements performed by organic liquid scintillation detectors. Liu et al. extracted the frequency-domain features by frequency gradient analysis (FGA) [13, 14] which exhibited a strong insensitivity to the variation in pulse response of the PMT. The FGA method exploits the difference between the zero-frequency component and the first frequency component of Fourier transform of the acquired signal and combines the advantage of insensitivity to noise associated with spectral analysis with that of the real-time

Received 17 April 2013
* Supported by National Natural Science Foundation of China (11175254)
1) E-mail: jyang@nudt.edu.cn

implementation of the PGA algorithm. However, for the pulse shapes produced at the output of a liquid scintillator are non-stationary signals, their analysis using conventional Fourier transform could not capture their most relevant features. Yousefi et al. adopted a new PSD method based on the wavelet transform [15, 16] to discriminate neutrons and γ, rays which presented an efficient tool to analyze non-stationary signals. Experimental results show that compared with the PGA algorithm, the wavelet-based method provides an improvement in reducing the overlap between neutron and γ-ray events reflected by an increase in the FOM. Besides, other methods, such as artificial neural networks [17] and the fuzzy c-means algorithm [18] have been investigated with varying degrees of success.

In this paper, we propose a new PSD method based on wavelet transform modulus maximum (WTMM) which is able to discriminate neutrons and γ rays in liquid scintillators. This method exploits the contractive trend between the positive modulus maximum curve and the negative modulus maximum curve in the wavelet-domain. In addition, since the WTMM method itself was presented to eliminate the noise, based on the different properties of signals and noise with wavelet transform, there is no need to make any pretreatment to the signals. Moreover, it is verified with characterization of these events arising from the measurement of time of flight (TOF). The TOF technique has previously been used to compare digital and analogue methods of discrimination and to measure the degree of discrimination quality on a quantitative basis. In this research, it has been used to check the performance of the WTMM method. Detailed principle of discrimination with WTMM and the simulation results are given in Section 2; the experimental set-up and the comparison with the CC method and the WTMM method are given in Section 3; the conclusions arising from this research are given in Section 4.

2 The principle of the WTMM discrimination method

2.1 Wavelet transform and modulus maximum theory

In the case of nuclear pulse signals, as pulse parameters vary in time and within an ensemble of different pulses, it can be concluded that the process we are dealing with must be considered as non-stationary. In order to analyze this type of pulse, the wavelet transform (WT) uses short time windows at high frequencies and long time windows at low frequencies. Accordingly, the WT provides versions of some parameter estimation at different observation scales. This type of transform converts a function of time, $f(t)$, into a function of two variables: scale and time, $W_{\rm f}(a,t)$. By evaluating the convolution of the useful and the scaled version of the prototype wavelet, $\varphi_a(t)=a^{-1/2}\varphi(t/a)$, the transform at different scales may be obtained

$$W_{\rm f}(a,t)=f(t)*\varphi_a(t)=\frac{1}{\sqrt{a}}\int_{-\infty}^{+\infty}f(b)\varphi^*\left(\frac{t-b}{a}\right)\mathrm{d}b. \quad (1)$$

From the point of view of signal response, wavelet transform can be considered as the impulse response of $\varphi_a(t)$. Suppose the wavelet $\varphi_a(t)$ and the signal $f(t)$ to be analyzed are both real functions, and a point $(a_0,\ t_0)$ in a given scale $a=a_0$, satisfies

$$\frac{\partial W_{\rm f}(a,t_0)}{\partial t}=0. \quad (2)$$

We call it the local maxima point. Then local modulus maxima at points $(a_0,\ t_0)$ can be defined such that

$$|W_{\rm f}(a_0,t)|\leqslant|W_{\rm f}(a_0,t_0)|, \quad (3)$$

where t is either the right or the left neighborhood of t_0. Therefore, at a given scale a_0, a set of modulus maxima can be obtained from the coefficients. Maxima curves are defined as those curves connected by arbitrarily close points in the time-scale plane, along which all points are modulus maxima. For singularity detecting, the derivative of the 'Gauss function' is generally chosen as the prototype wavelet to assure modulus maximum curves spread to the least scale [19]. In this research, the first derivative of 'Gauss function' wavelet was used.

2.2 The discrimination theory of neutron and γ ray based on WTMM

Reference [20] has indicated that the Lipschitz exponent of a Dirac delta function is $\alpha=-1$. Both the normalized neutron waveform and the γ ray waveform are similar to the Dirac delta function, so their Lipschitz exponents will be close to -1. However, the decay trend of γ-ray pulse is faster than that of a neutron pulse, i.e. the γ-ray waveform is 'more similar' to the delta function than the neutron waveform, which results in that the Lipschitz exponent of the γ-ray pulse is 'more close' to -1 than that of the neutron pulse. This slight difference of characteristic information carried by the neutron pulse waveform and the γ-ray pulse waveform will be used to discriminate between them.

To make the above statements clear, the continuous wavelet transform is computed first. Typical neutron and γ-ray waveforms with their corresponding modulus maximum curves are plotted in Fig. 1. Fig. 1(a) and (b) are the normalized pulse of neutron and γ ray obtained from Marrone's model [21] with a sampling number of 1024 at sampling rate 5 G/s. Figs. 1(c) and (d) show the continuous waveform function, the bright regions indicate the positive modulus maximum points, while the dark ones are negative modulus maximum points; Figs. 1(e) and (f) are the modulus maximum curves extracted from (c)

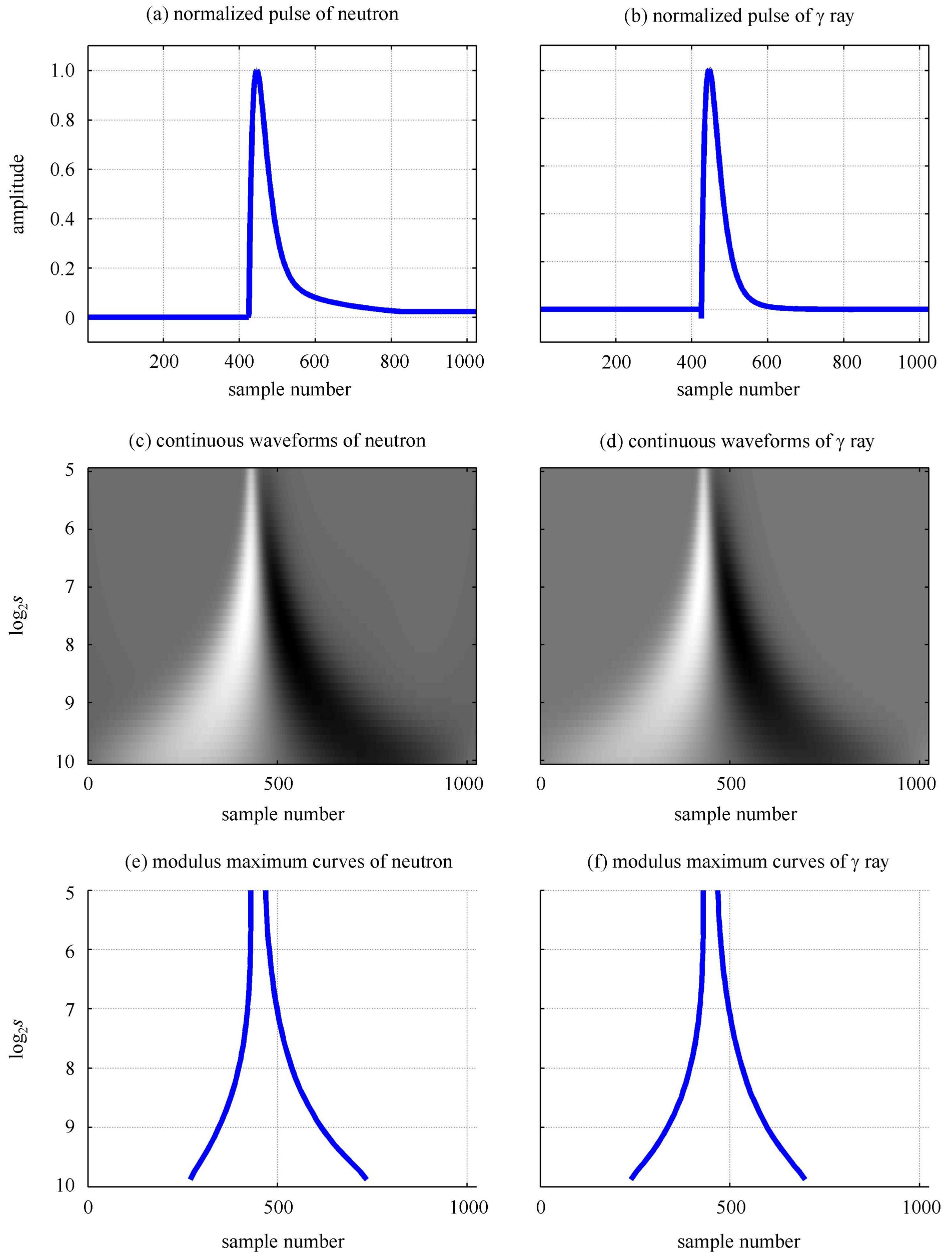

Fig. 1. (color online) Typical neutron and γ-ray waveforms with their corresponding modulus maximum function.

and (d), respectively.

Secondly, the corresponding wavelet coefficients versus scale of the function are shown in Fig. 2. The modulus maximum curves of typical neutron and γ ray are inconspicuous in the scale-time plane, so we move them to the scale-space plane, whose horizontal coordinate is the logarithm of scale, while the vertical coordinate is the logarithm of modulus maximum.

We approximately obtain Lipschitz exponents by the curve fitting of a polynomial of degree 1 to each line to calculate the decay ratio in Fig. 3 as $\alpha_{\text{n}-\min}=-0.686$, $\alpha_{\text{n}-\max}=-0.788$, $\alpha_{\gamma-\min}=-0.846$, $\alpha_{\gamma-\max}=-0.891$, which accord with the above statements. These calculation results verify the feasibility of the discrimination method based on WTMM. However, the calculation of the Lipschitz exponent is not easy, although taking the Lipschitz exponent the discriminating parameter has a clear meaning.

From Fig. 2, we can discover that there are distinct differences between the asymptotic decay trend areas of the γ-ray signal and the neutron signal, which can be used as prominent features to discriminate them, so we define a new parameter, i.e. MMT called the 'Modulus Maximum Trend', to discriminate neutron and γ ray as

$$\mathrm{MMT} = \int_{\log_2 s} (\log_2 |W_{\mathrm{f}}(a,t)|_{\max} - \log_2 |W_{\mathrm{f}}(a,t)|_{\min}) d(\log_2 s). \quad (4)$$

The defined MMT is equal to the enwrapped area of the modulus maximum curves belonging to neutron or γ ray, as shown in the shadows of Fig. 3.

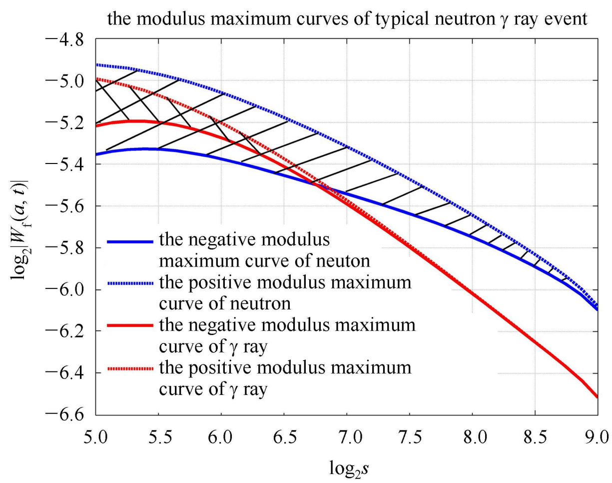

Fig. 2. (color online) The modulus maximum curves of typical neutron and γ ray. The blue lines belong to the neutron, and the red lines belong to the γ ray.

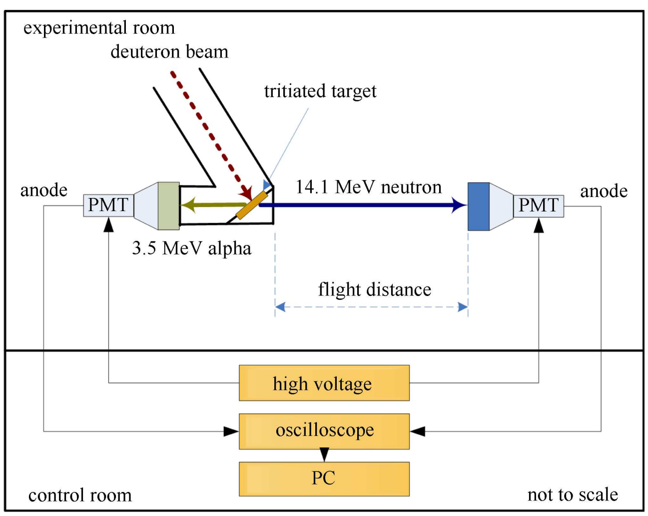

Fig. 3. (color online) A schematic of the experimental set-up used for the associated particle neutron generator at the Institute of Nuclear Physics and Chemistry, the Chinese Academy of Engineering Physics, Mianyang, China.

Finally, we investigate the robustness of the WTMM method by adding white noise. The result shows, with decreasing of SNR less than 11 dB, the error ratios of neutron and γ ray deteriorate sharply. In those conditions, the properties of signal and noise with wavelet transform in the scale domain are unconspicuous, the modulus maximum curves of the signal are fluctuated by the modulus maximum curves of noise, and then the WTMM method cannot be successfully utilized to classify neutron and γ-ray events.

3 Experimental results and discussion

3.1 Experimental set-up

The experimental data analyzed in this work were acquired using the TOF measurement system at the Institute of Nuclear Physics and Chemistry, the Chinese Academy of Engineering Physics, Mianyang, China. As shown in Fig. 3, through deuterium-tritium fusion reaction, an associated particle neutron generator (APNG) produces neutrons and alpha particles that are correlated in time and travel in opposite directions to conserve momentum. The energies of neutrons and alpha particles are 14.1 MeV and 3.5 MeV, respectively. More details of the experimental set-up can be referred to Ref. [14].

In our research, the distance between the liquid scintillation detector BC501A and tritiated target, i.e. the flight path length, was set as 1000 mm. The liquid scintillator pulse and the corresponding beam-pickup pulse data are captured digitally with a sampling rate of 5 G Samples/s and 8-bit amplitude resolution. A total of 3679 events were recorded and analyzed. The results of the TOF method are given in Table 1.

Table 1. Experimental results of TOF. There are a total of 3679 events.

TOF assignment	neutrons	γ rays	scatter
number	2133	1449	97

3.2 Experimental results and discussion

The total 3582 pulses induced by neutron or γ-ray events are applied to the WTMM and the CC method to verify the feasibility of each method respectively. The results are shown in Fig. 4 and Fig. 5. The results of this analysis are given in Table 2.

Table 2. The discrimination results of the WTMM method and the CC method.

method	n	γ rays	FOM
WMMT	2121	1433	1.382
CC	1989	1343	1.178

Traditionally, the Figure of Merit (FOM) of a discrimination method has relied upon the calculation of a single figure which is used to identify interaction type by

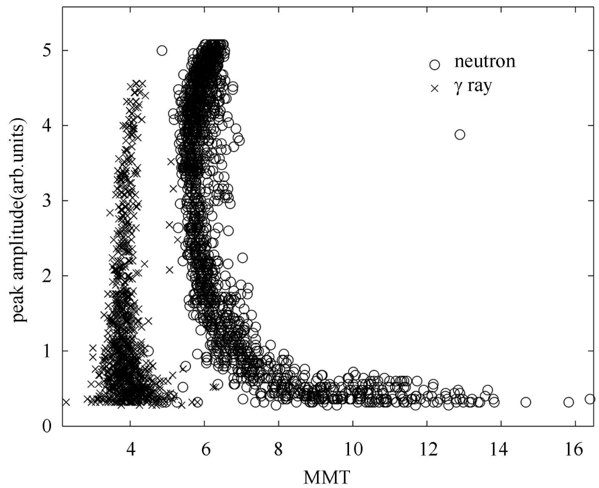

Fig. 4. A total of 3582 events are discriminated by WTMM. The horizontal coordinate is MMT, and the vertical coordinate is the peak amplitude of each pulse.

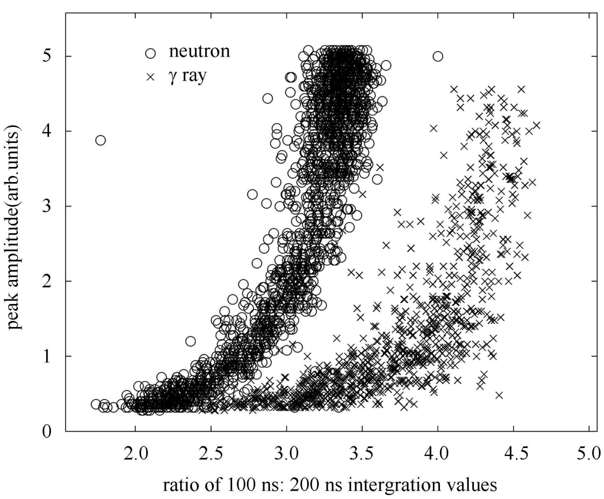

Fig. 5. A scatter of the peak amplitude against the ratio of 100 ns:20 ns integration values of the CC method are applied to 3582 events.

simple bounds checking, e.g., if the discrimination figure is over a certain value then it is a particular interaction type. The FOM is then calculated by

$$\mathrm{FOM}=\frac{S}{\mathrm{FWHM_n}+\mathrm{FWHM}_\gamma}, \tag{5}$$

where S is the separation between the centroids of the neutron peak and the γ-ray peak in the spectrum, and $\mathrm{FWHM_n}$ and FWHM_γ are the full Width at half maximum values of the two peaks of this fit. Fig. 6 shows the distribution for the WTMM discrimination plane together with the double Gaussian fit. The FOM results of the WTMM method and the CC method are also shown in Table 2.

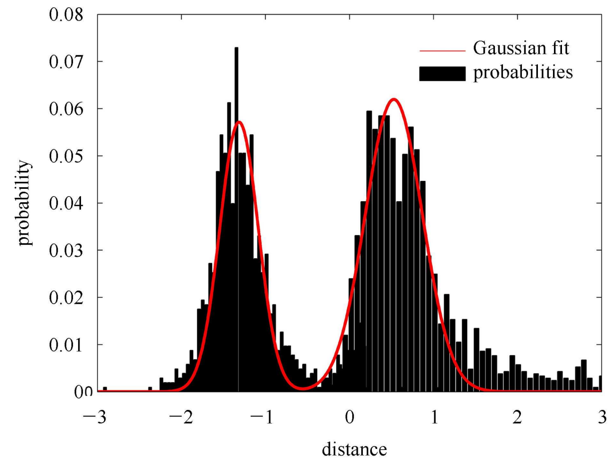

Fig. 6. (color online) The distribution of the distance from the mean line between the centroids (of the neutron and γ ray plumes) and each point in WTMM discrimination plane.

The discrimination results of the WTMM method and the CC method are shown in Table 2. The FOMs of CC and WTMM are calculated as $\mathrm{FOM_{CC}}$=1.178 and $\mathrm{FOM_{WTMM}}$=1.382, respectively. For the FOM results, the FOM of WTMM is about 17.3 percent larger than that of CC, which indicates an improvement of the performance over CC in discriminating neutrons and γ rays. Moreover, according to the data in Table 2, there are some slight differences in the numbers of each event identified by them and the experimental results obtained from WTMM are slightly closer to those of TOF. For example, the total number of neutron events arising from TOF, CC and WTMM are 2133, 1989 and 2121, respectively. There are 144 neutron events mistakenly classified as γ-ray events by CC, whilst there are only 12 neutron events being mistakenly classified as γ-ray events by WTMM. Comparing the FOMs in Table 2, the WTMM method appears to be an improvement over the CC method in terms of its discrimination capabilities.

The CC algorithms used in this experiment use a 47 points moving average filter before further process and present poor stability. Whereas the WTMM method developed in this research uses no filter and exhibits a strong insensitivity to noise. In this regard, the WTMM is an optimization over the CC algorithm in terms of robustness.

All these analyses indicate directly that the wavelet transform method excelled over the CC method in discriminating neutron and γ ray.

4 Conclusions

Given the distinct differences of the asymptotic decay trends between the positive modulus maximum curve and the negative modulus maximum curve of neutron and γ-ray signals, which can be used as prominent features to discriminate between them, a novel discrimination method based on the wavelet transform called the WTMM method has been proposed. Its discrimination performance has been studied and compared with the TOF method and the CC method. Theoretical and experimental results show that the WTMM method exhibits a strong insensitivity to the variation in pulse response of the PMT and the electronic noise and therefore takes possession of a better performance than other discrimination methods.

However, the overheads of calculating this wavelet-based PSD method are heavier than other methods and hence it is not suitable for general real-time embedded systems. However, as the configurable embedded systems continue to develop in capability and speed, the relative merits of wavelet-based methods will be dependent on the elegance with which they are implemented.

We acknowledge the support of the Institute of Nuclear Physics and Chemistry, the Chinese Academy of Engineering Physics, Mianyang, China. We also appreciate the help and advice of Dr. X. Ma at the Department of Engineering, Lancaster University, U.K.

References

1 Knoll G F. Radiation Detection and Measurement. Third edition. New York: Wiley, 2000

2 Brooks F D. Nucl. Instrum. Methods, 1959, **4**: 151–163

3 Adams J M, White G. Nucl. Instrum. Methods, 1978, **156**: 459–476

4 Alexander T K, Goulding F S. Nucl. Instrum. Methods, 1961, **13**: 244–246

5 Roush M, Wilson M A, Hornyak W F et al. Nucl. Instrum. Methods, 1964, **31**: 112–114

6 Moszyńki M, Costa G J et al. Nucl. Instrum. Methods A, 1994, **350**: 226–234

7 Jastaniah S D, Sellin P J. Nucl. Instrum. Methods A, 2004, **517**: 202–210

8 Cerný J, Doležal Z et al. Nucl. Instrum. Methods A, 2004, **527**: 512–518

9 Mellow B D, Aspinall M D et al. Nucl. Instrum. Methods A, 2007, **578**: 191

10 Aspinall M D, Mellow B D et al. Nucl. Instrum. Methods A, 2007, **583**: 432–438

11 Joyce M J, Aspinall M D et al. IEEE Trans. Nucl. Sci. 2010, **57**: 2625–2630

12 Marrone S, Cano-Ott D et al. Nucl. Instrum. Methods A, 2002, **490**: 299

13 LIU G, Joyce M J, MA X et al. IEEE Trans. Nucl. Sci. 2010, **57**: 1682–1691

14 YANG J, LUO X et al. Chinese Physics C, 2012, **36**(6): 544–551

15 Yousefi S, Lucchese L et al. Nucl. Instrum. Methods A, 2009, **598**: 551–555

16 Shippen D I, Joyce M J et al. IEEE Trans. Nucl. Sci. 2010, **57**: 2617–2625

17 LIU G, Aspinall M D et al. Nucl. Instrum. Methods A, 2009, **607**: 620–628

18 Savran D, Loher B et al. Nucl. Instrum. Methods A, 2010, **624**: 675–683

19 Mallat S. A Wavelet tour of Signal Processing. SanDiego, CA: Academic Press, 1997

20 Mallat S, Hwang W. IEEE Transactions on Information Theory, 1992, **38**: 617–643

21 Aspinall M D, Mellow B D et al. Nucl. Instrum. Methods A, 2007, **578**: 261